The Flux Monitor
(Technical Note)

M. Bashkanov,* D. P. Watts, and N. Zachariou
Department of Physics, University of York, Heslington, York, Y010 5DD, UK

E. Chudakov and H. Egiyan
Thomas Jefferson National Accelerator Facility, Newport News, VA 23606, USA

M. Amaryan
Old Dominion University, Norfolk, VA 23529, USA

S. Dobbs
Florida State University, Tallahassee, FL 32306-4350, USA

J. Ritman
Institut für Experimentalphysik I - Ruhr-Universität, Bochum 44780, Germany

J. R. Stevens
College of William and Mary, Williamsburg, VA 23185, USA

I. Strakovsky
The George Washington University, Washington, DC 20052, USA

(Dated: July 18, 2023)

* mikhail.bashkanov@york.ac.uk

CONTENTS

Abstract. An accurate determination of the K_L beam flux is necessary to maximise the physics impact of the KLF data. During the proposal stage, several versions of the Flux Monitor were considered. We have finally agreed on the least risky and the most affordable design, which can be extended or upgraded at any future point if additional resources are available. This design uses several decommissioned components of the WASA-at-COSY detector, and has room for an optional solenoidal magnet. The current design allows the reconstruction of the Kaon beam flux with an accuracy of 5% over the full KLF momentum range. For the beam momentum range relevant to hyperon spectroscopy, the statistical accuracy of the flux determination of better than 1% is achievable within a day.

I. K_L FLUX MONITORING

An accurate determination of the K_L beam flux is necessary to maximise the physics impact of the KLF data. To reach an accuracy of $< 5\%$ in the determination of the K_L flux we plan to build a dedicated Flux Monitor (KFM). This device will provide a significant improvement over the typical 10% accuracy achievable from normalisation of the data to previously measured reactions, for instance, $K_L p \to K_S p$.

The design of a KFM could employ the regeneration of K_S and detection of $\pi^+\pi^-$ pairs in a Pair Spectrometer as done at Daresbury [1]. However, this technique affects the quality of the resulting K_L beam. Therefore, a more effective choice for the KFM at JLab would utilise in-flight decays of the K_L. The K_L has four dominant decay modes [2]:

- $K_L \to \pi^+\pi^-\pi^0$ BR = 12.54% .
- $K_L \to \pi^0\pi^0\pi^0$ BR = 19.52% .
- $K_L \to \pi^\pm e^\mp \nu$ BR = 40.55% .
- $K_L \to \pi^\pm \mu^\mp \nu$ BR = 27.04% .

All decay modes with two charged particles in the final state can be used for flux determination. However, in this memo we will concentrate on the simplest decay, $K_L \to \pi^+\pi^-\pi^0$, where both charged particles have the same mass.

II. FLUX MONITOR LOCATION

To account for various possible acceptance effects during K_L beam propagation from the Be target, we plan to measure the K_L flux upstream of the GlueX detector, utilising the Hall D Pair Spectrometer as shielding against K_L which have decayed further upstream. As seen from the Figure 1, our current design of the KFM fits in the available space downstream from the GlueX pair spectrometer magnet very well. The only equipment which needs to be moved prior to the KFM installation are the two arms of the Pair Spectrometer and the shielding wall.

III. FLUX MONITOR COMPONENTS AND ACCEPTANCE

All the K_L beam decay products are very forward peaked, but one needs to have a large acceptance to reconstruct K_L distributed along the length of the 24 m K_L beamline. The KFM design proposed and described in this memo will measure a small fraction of decayed K_L's, concentrating on the portion decaying within a distance of 2 m downstream of the pair spectrometer magnet centre, Fig. 1. The Flux Monitor described in this memo consists of the following major parts from upstream to downstream: the Start detector (Fig. 3), the forward tracker, the backward tracker (Fig. 5), and the Stop detector (Fig. 4). An optional solenoid magnet from a used MRI (Fig. 7) can be placed in between the trackers.

To measure the decays of these K_L's, a detector system of roughly 50 cm diameter is sufficient, however, since we will reutilise existing components, the KLM will cover a larger range. In particular, the proposed components will extend over a 75 cm diameter at the "Start station" and $\sim$ 2.5 m diameter at "Stop station." The optional MRI magnet has a 70 cm bore. On Figure 2 one can see an acceptance for a 70 cm diameter system for various decay branches as a function of K_L beam momentum. The 3π decay branch has sizeable and reasonably uniform acceptance over the full range of K_L.

The Start detector consists of a pizza-piece shaped segmented double-layer plastic scintillator, the former WASA-at-COSY Forward Window Counter used to provide start timing signals for time-of-flight (ToF) as well as signals for the trigger electronics. Each layer has 24 elements and is built of 3 mm thick BC408 plastic scintillator coupled to XP1312 PMT from Phonics with twisted adiabatic lightguides. All PMT's are housed in individual μ-metal cylinders

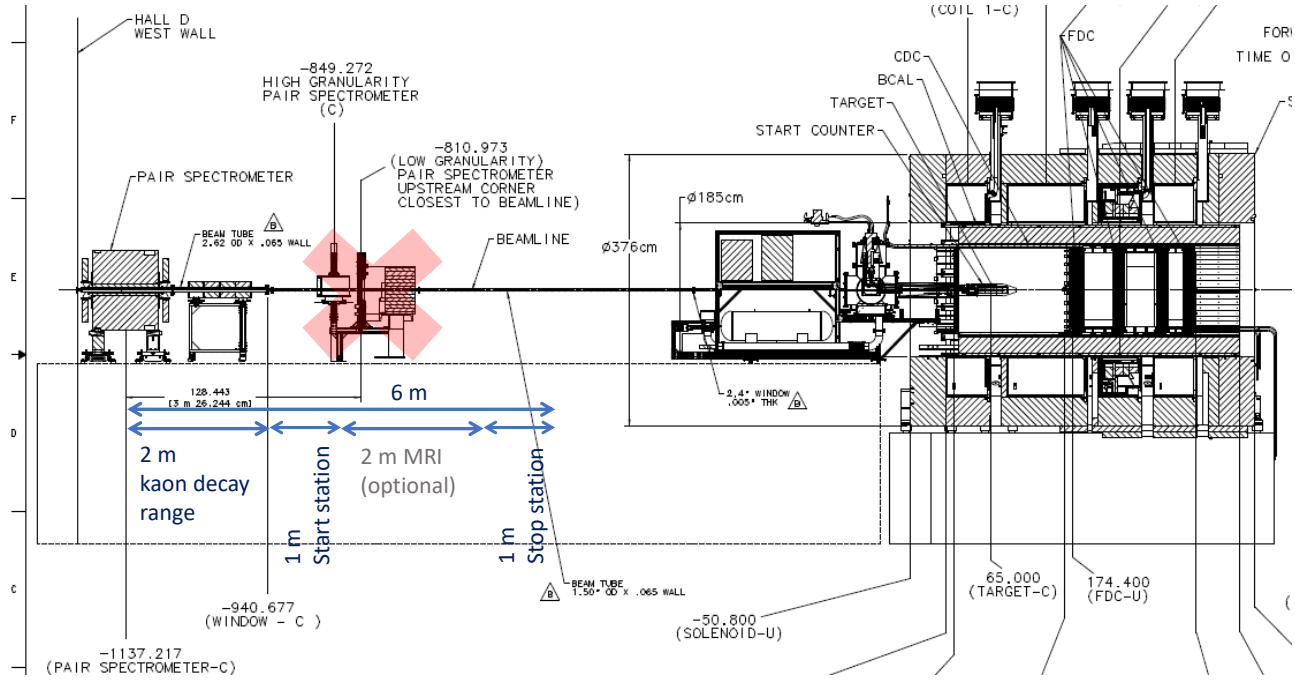

FIG. 1. The Flux Monitor Location in Hall D. The red cross indicates to the pair spectrometer, which needs to be removed prior to KFM installation.

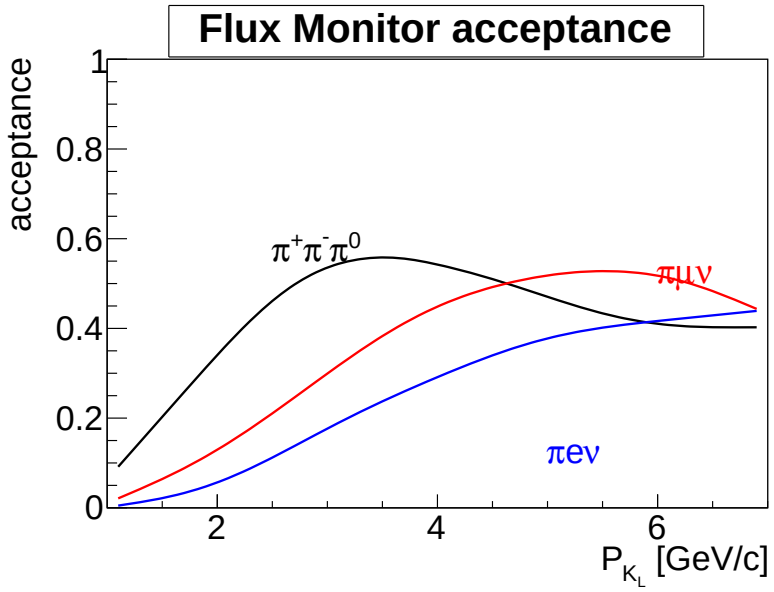

FIG. 2. The Flux Monitor acceptance for various decay K_L branches.

to shield from magnetic field. Further details can be found in Ref. [3]. Dimensions of the supporting structures are also shown in Appendix A. This detector is available for use starting from Q4 2023. The detector has 75 cm diameter active area and 0.16 ns time resolution [3] which exceed the KFM requirement.

The Stop detector has a "wall" design, made of 24 bars 20 mm thick and 120 mm wide. Details of the Stop detector geometry can be seen on Fig. 4. Further details can be found in Ref. [3]. The Stop detector bars consist of Eljen

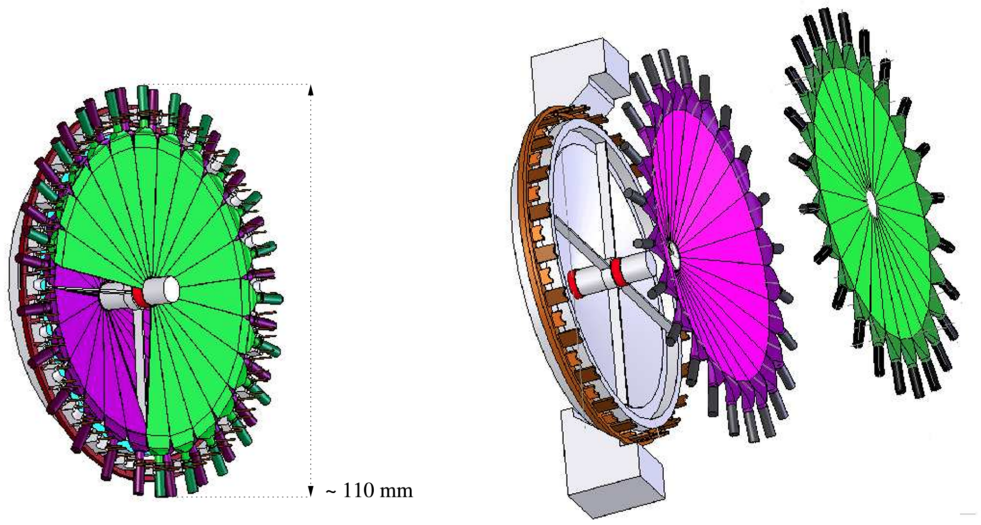

FIG. 3. The Start detector.

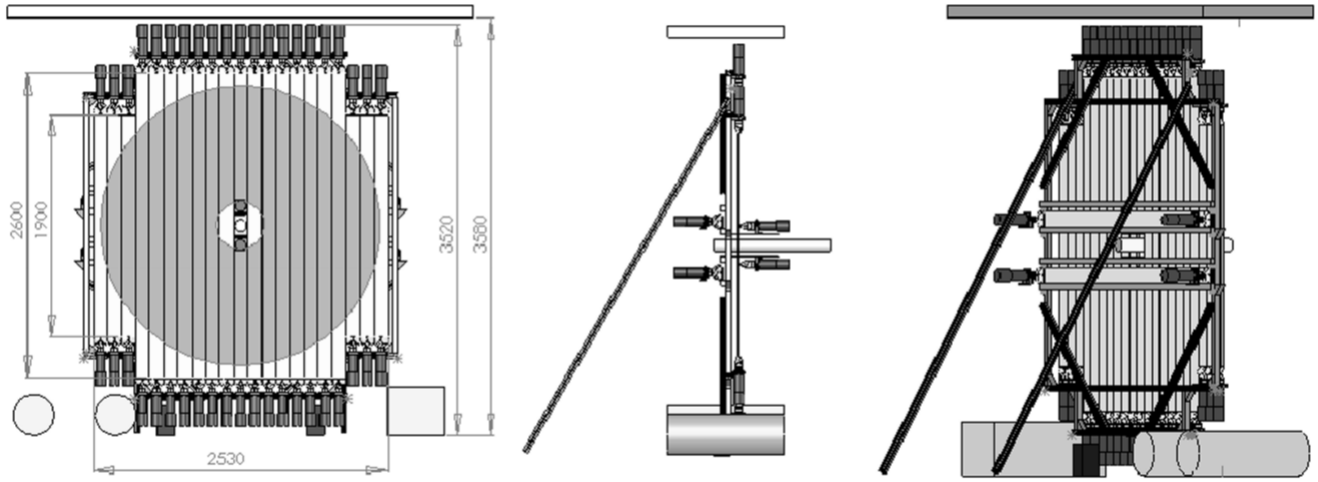

FIG. 4. The Stop detector.

EJ200 plastic scintillator coupled to XP2020C PMT's with twisted adiabatic lightguides read out from both sides of the bar. All PMT's are housed in 10 mm thick μ-metal housings to minimise the influence of magnetic field on electron showers. To simplify time calibration, the Stop detector is equipped with two additional horizontal scintillating bars sitting close to the beampipe, behind the main "wall." The two-side readout allows to reconstruct hit position along the bar by time difference along the detector ($\sigma \sim 3$ cm). However, since position of the hit will be measured by the tracker right before the wall with much higher accuracy < 1 mm a further improvement in time resolution is achievable.

The KFM tracker will be a four quatro-layered straw tube tracking system, using the former WASA-at-COSY Forward Proportional Chamber (FPC). It is composed of 4 identical modules, each with 4 staggered layers of 122 proportional drift tubes (so-called straws) of 8 mm diameter. The design of the detector and the attached electronics is made such as to preserve the option of charge division readout for obtaining information about the longitudinal hit position along the sense (anode) wire. Hence, a resistive wire of 35 μm thick stainless steel is used as the anode wire. The tracker uses a 50/50 Ar/CO_2 gas mixture and has a 35 μm position resolution. Further details about FPC can

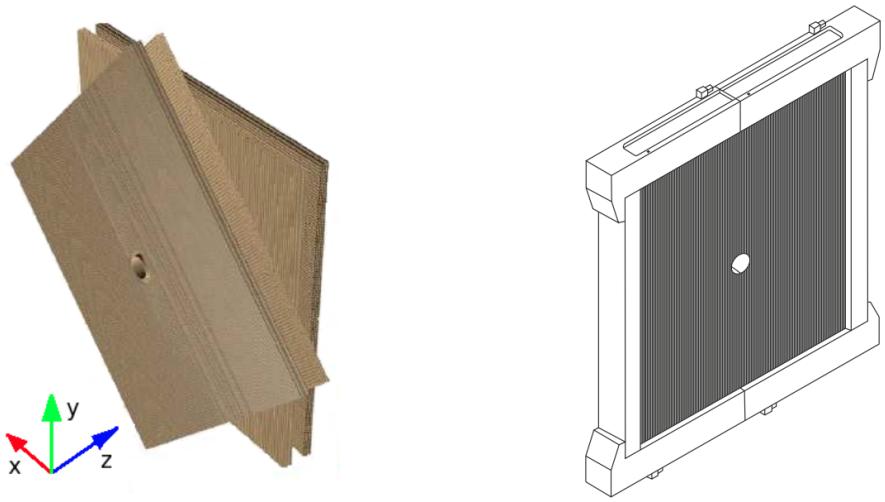

FIG. 5. Schematic view of the tracker. A three dimensional view of four modules of tracker(left) and the single tracker module in a frame(right)

be found in Ref. [4] and refs within.

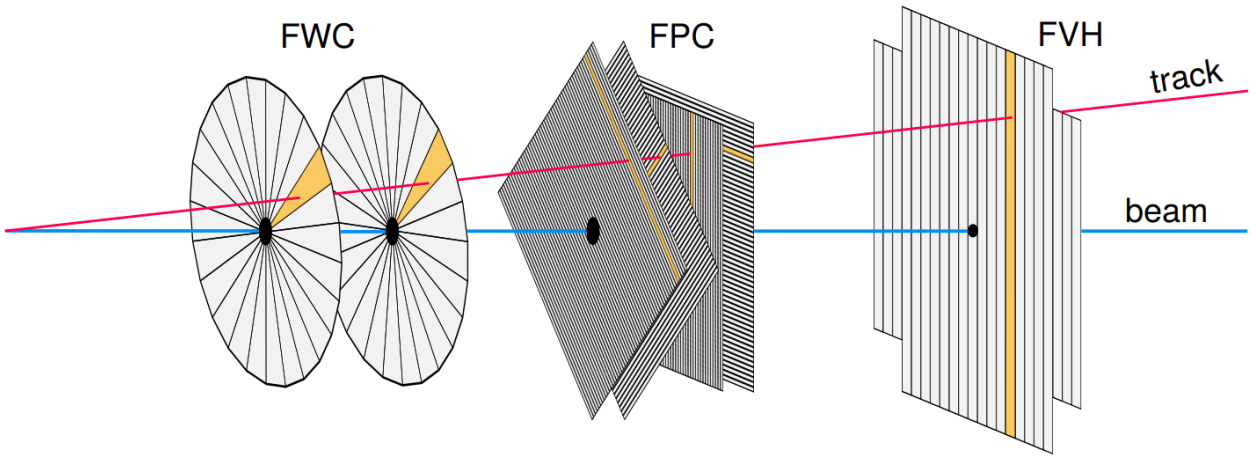

FIG. 6. The original WASA-at-COSY setup of start-stop and tracker systems.

In the original tracker design, the 4 modules were arranged as X-Y-V-W planes tilted by 45 degree relative to each other, see Fig. 6. In the KFM design, we plan to arrange modules in two double-layer (X-Y) stations separated by 2 m The upstream station is located right after the Start detector and the downstream station right before the stop. This arrangement has two reasons: to increase the lever arm and hence increase kaon decay vertex z-position resolution, and to accommodate the optional solenoid MRI magnet, Fig. 7.

The first implementation of a used MRI machine as a solenoid magnetic spectrometer can probably be traced to ISOLDE-ISS setup. Indeed, there is a large market of used MRI's where old, but working machines can be accessed at rather low price. The magnets of old MRI's might be considered rather weak ($1.5-3$ T) by today's standards, but they are usually sufficient for scientific purposes. On top of it, MRI's are equipped with off-the-shelf shimming as well as very reliable low maintenance cost cooling systems. All these things make the use of refurbished MRI as a magnetic solenoid spectrometer very appealing. A magnetic spectrometer is not essential for the kaon flux extraction. However, the use of the additional magnetic spectrometer simplifies the flux analysis by suppressing unwanted backgrounds with additional particle identification through the momentum vs. ToF technique, and it can enhance the programme

FIG. 7. The "optional" used MRI system to be used as a solenoid spectrometer.

by accessing physics beyond the standard model in rare kaon decays.

The components of the WASA-at-COSY detector discussed here, including electronics, were designed to sustain high-rate conditions of pp-collisions to access physics beyond the standard model via rare meson decays. The electronics was able to record more than 20k events per second and detectors operated properly with $\sim 10^7$ track per second rate. These conditions exceed the KFM requirements by several orders of magnitude.

IV. K_L FLUX DETERMINATION

The K_L flux has a complex dependence on momentum, transverse position and distance from the Be-target. Due to the $1/z^2$ solid angle suppression (here z is the distance from the Be target), the KFM would see 4 times more kaons than the LH_2/LD_2 cryogenic target in the main GlueX spectrometer. Also some kaons can decay on the way to the LH_2/LD_2 target. The flux suppression factor due to K_L decay is equal to $f(\beta) = e^{-\frac{Z}{c\tau\beta\gamma}}$, where $c = 29.9$ cm/ns is the speed of light, $\tau = 51$ ns is the K_L mean lifetime; $\beta = v/c$ – kaon velocity in units of speed of light; $\gamma = 1/\sqrt{1-\beta^2}$. Because of these dependencies accurate flux monitoring requires determination of the kaon flux as both a function of transverse position within the beampipe and Kaon energy. A 7 cm diameter beam pipe allows sufficient margins for the clean definition of a fiducial regions for the transverse beam profile at the KFM position. One should also keep in mind that the radial extent of the kaon beam varies with kaon momentum, as fast kaons tend to be more focused due to the larger Lorentz boost. All in all, we expect to measure about 4.5k Kaon/s in the KFM. In Figure. 8, one can see the Kaon flux experienced by the FM and by the LH_2/LD_2 target respectively. The increased yield of low-momentum Kaons observed in the KFM compared to at the cryogenic target arises because these low momenta particles have a larger possibility of decaying in the KFM, and many decay before reaching the cryogenic target.

For the K_L decay products to be measured by the KFM, both charged particles from the kaon decay need to be incident within the KFM acceptance, see Figure 2. Taking into account the different branching ratios and decay kinematics, we expect to reconstruct the following number of K_L from various decay channels, see Figure 9.

One can quantify the expected rate in terms of the achievable statistical error within a one day measurement (Figure 10 left) and the number of days required to get a 1% statistical accuracy in flux (Figure 10 right) for a

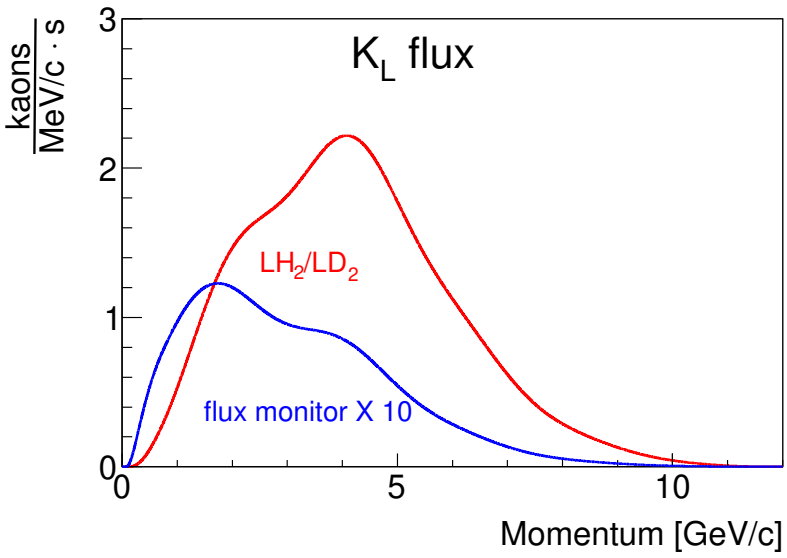

FIG. 8. Kaon flux at LH_2/LD_2 target (red) and at KFM (blue). The yield of events from the KFM is multiplied by 10.

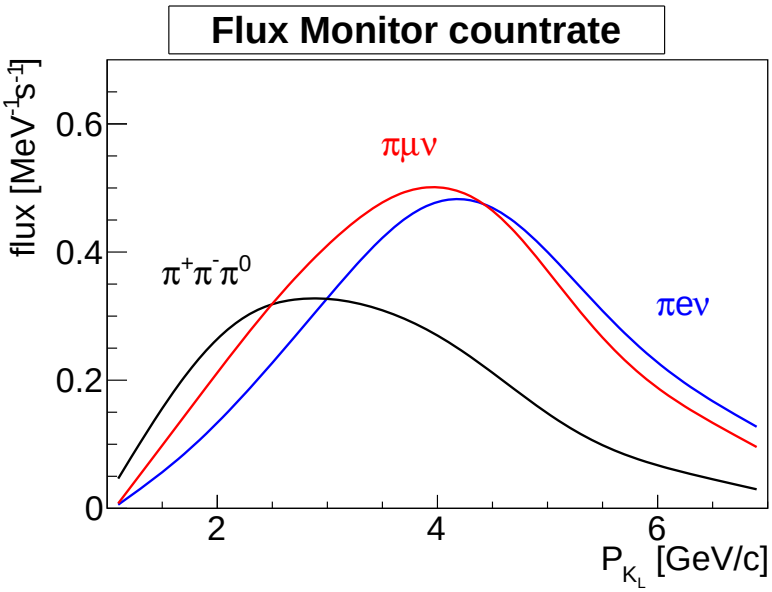

FIG. 9. Visible K_L flux for various decay channels within the FM acceptance.

20 MeV/c bins in K_L momentum when analyzing the $\pi^+\pi^-\pi^0$ decay.

For the kaon beam momenta range appropriate for the hyperon programme ($\sim 1-5$ GeV/c) a 1% statistical error of the K_L flux determination is achievable in less than a day. The kaon flux analysis described in this section will be performed offline on a weekly basis, with possible daily crosschecks if the online monitoring described below shows any hints for unstable beam behaviour.

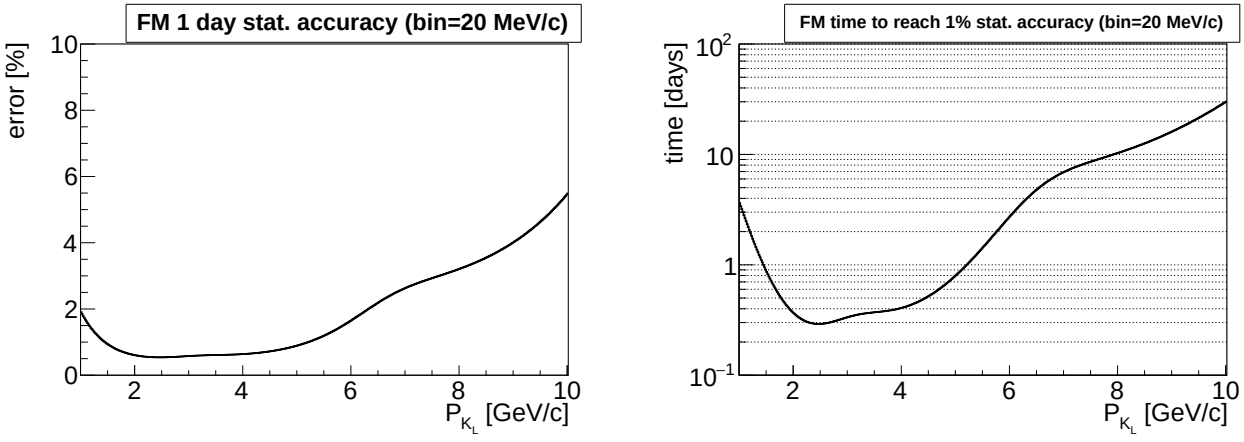

FIG. 10. Expected statistical accuracy for 1 day FM measurement (left) and time to reach 1% accuracy (right) for 20 MeV/c bins in K_L momentum and $\pi^+\pi^-\pi^0$ decay branch.

V. VERTEX POSITION RECONSTRUCTION

To reconstruct the spatial distribution of the K_L flux within the beam pipe as well as to determine the K_L time-of-flight from the Be-target, an accurate reconstruction of the K_L decay vertex position is required. The accuracy of vertex reconstruction depends solely on the accuracy of the tracking modules. With the tracker module described above (the former WASA-at-COSY FPC), we can achieve the following resolution. In our simulations, we have assumed that both forward and backward tracking stations are made of X-Y modules with the distance between X and Y layers of 5 cm. The position accuracy which can be determined from each sub-module is assumed to be $d = 250$ μm. We performed simulations for both options: the default configuration (without magnetic field), and with the "optional" MRI solenoid magnetic field between the tracking stations. The vertex position in the transverse plane

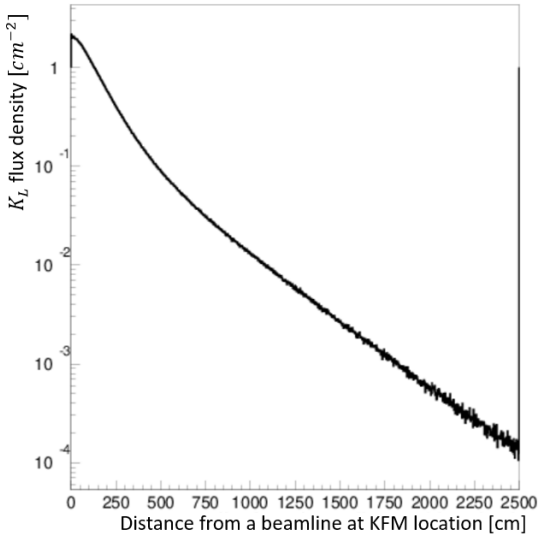

FIG. 11. Kaon flux density distribution in transverse direction at KFM location

is largely defined by the forward tracker, since the magnetic field skews tracks. However, the magnetic field does not change the polar angle (Θ), hence the position along the beam direction is largely defined by the forward-backward tracker difference. In our resolution studies we performed a two-track fit, assuming a common vertex, rather than making simultaneous track fits with vertex extraction from the distance of closest approach of the tracks. In the no-magnetic field mode (ToF mode, main option), both trackers contribute to the transverse position resolution. The

position resolution changes with distance and polar angle: the closer to the tracker and the higher angle, the better the resolution. On average, one can say that K_L position resolution in the transverse plane is about $2 \cdot d \sim 0.5$ mm and in the longitudinal direction $\sim 20 \cdot d \sim 5$ mm, where $d = 250$ μm is the single plane tracker resolution. Even a $d = 1$ mm tracker resolution should allow a sufficient reconstruction of the beam profile. The K_L angular distribution is very broad (see Fig. 11), so the typical 250 μm resolution which we expect for the KFM tracker would be more than adequate for this application.

VI. DECAY RECONSTRUCTION

The different K_L decay modes measurement in the KFM will be primarily separated by time-of-flight measurements. There are several contributions to the time resolution in the current design. The Start detector has a time resolution of 160 ps, including electronics, and has a double-layered design, which can improve the resolution by $\sqrt{2}$. The Stop detector has somewhat worse time resolution of about 250 ps. Details of the WASA electronics used in the system can be found in Ref. [7]. The time processing is performed with FastTDC, based on GPX ASIC chip [6] and has an intrinsic resolution of 81 ps. The K_L decay vertex time resolution defines the achievable momentum resolution. We expect it to be better than a single track/single cap time resolution(Fig. 12), but for our simulations we have assumed a conservative 100 ps [8].

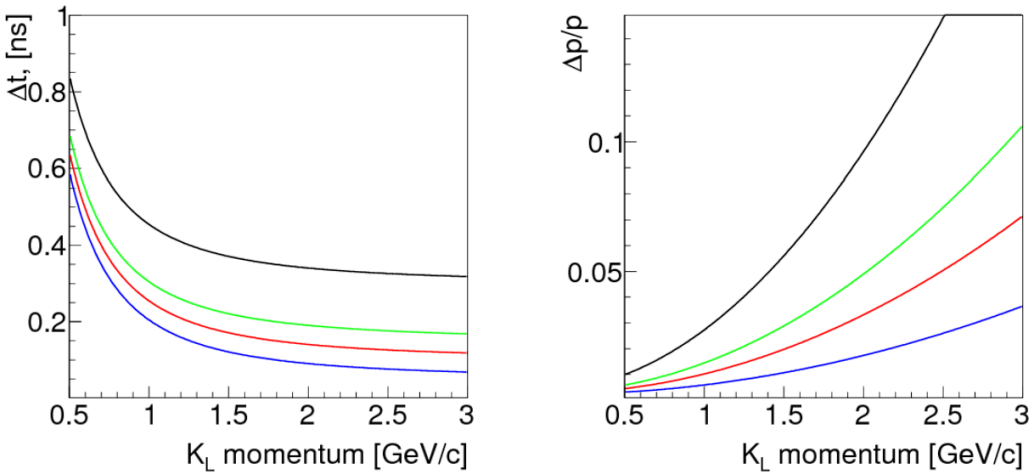

FIG. 12. Left plot: Time resolution, Δt, for K_L beam as a function of K_L momentum. Right plot: Momentum resolution, $\Delta p/p$, as a function of momentum. For 300ps (black), 150 ps (green), 100 ps (red), and 50 ps (blue) time resolutions.

The momentum resolution in a solenoid magnetic field is fully determined by the tracker resolutions. The displacement in solenoid magnetic field is equal to

$$d' \sim (l^2 \cdot z \cdot 0.3 \cdot B \cdot \sin\Theta)/(2 \cdot p) \, ,$$

where l is the length of the magnet [m], B is magnetic field strength [T], z is the particle charge, and p is momentum [GeV/c]. For the $l = B = z = 1$, we have

$$d' \sim (0.3 \cdot \sin\Theta)/(2 \cdot p) \, .$$

The magnetic field only acts on the transverse momentum component. For a typical momentum of 1 GeV/c and a 5 degree polar angle, a displacement of 13 mm is expected. For a 1 GeV/c and 1 degree polar angle a displacement would be the reduced to 2.6 mm (With a standard MRI $z = 1.8$ m and $B = 1.5$ T corresponding numbers would be 64 mm and 13 mm). Despite these limitations a magnetic field momentum reconstruction is expected to work a lot better than the ToF reconstruction. The expected performance of ToF and magnetic reconstruction is illustrated in Figure 13 (The simulation was performed with a realistic K_L momentum profile from Fig. 8).

Correct mass assignment for the $\pi^+\pi^-\pi^0$ decay compared to the semi-leptonic decays give a much narrower Missing Mass (MM) distribution. A 1-Dimensional projection to the y-axis, as shown in Figure 14 allows a direct comparison of various scenarios.

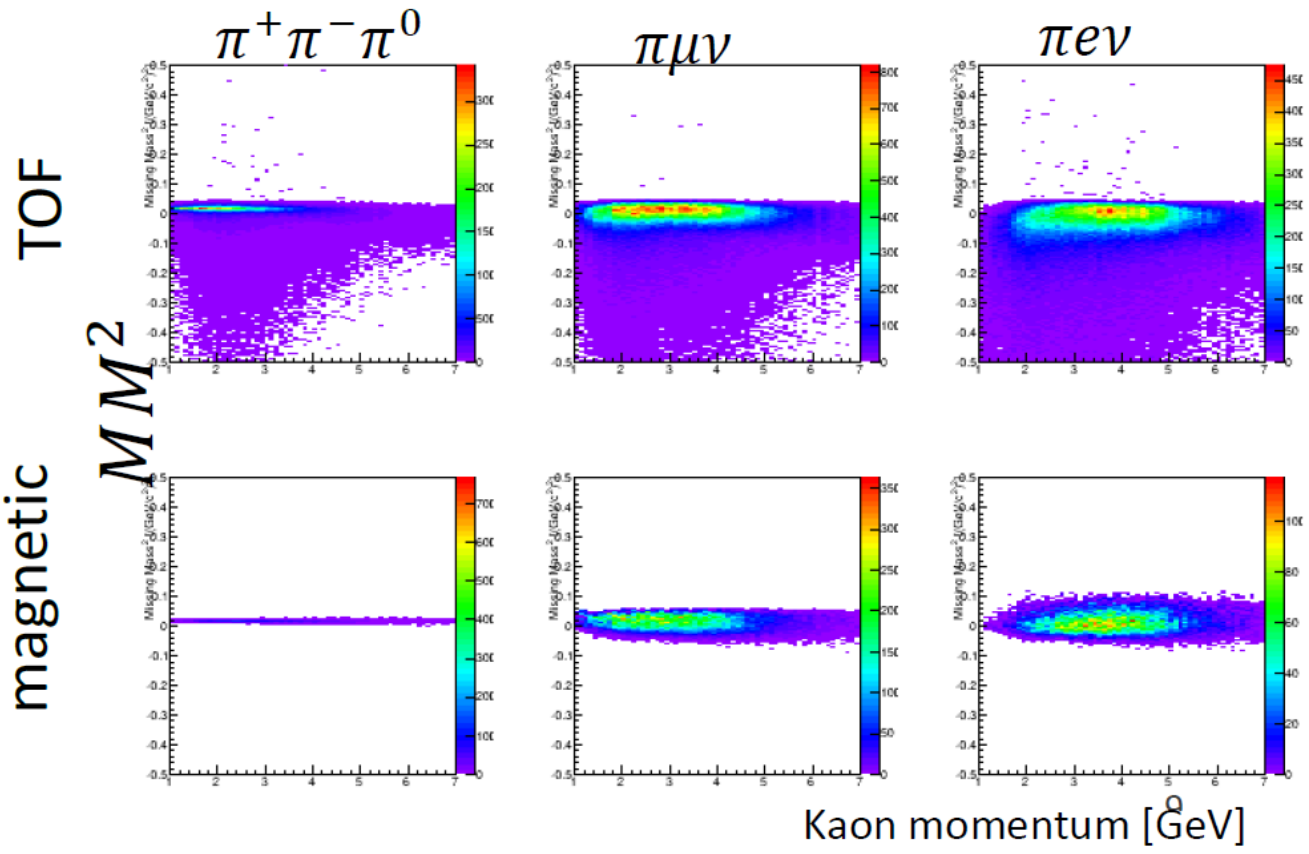

FIG. 13. Missing mass reconstruction with ToF and magnet as a function of kaon momentum. All charged particles in all decay channels are assumed to have mass of pion.

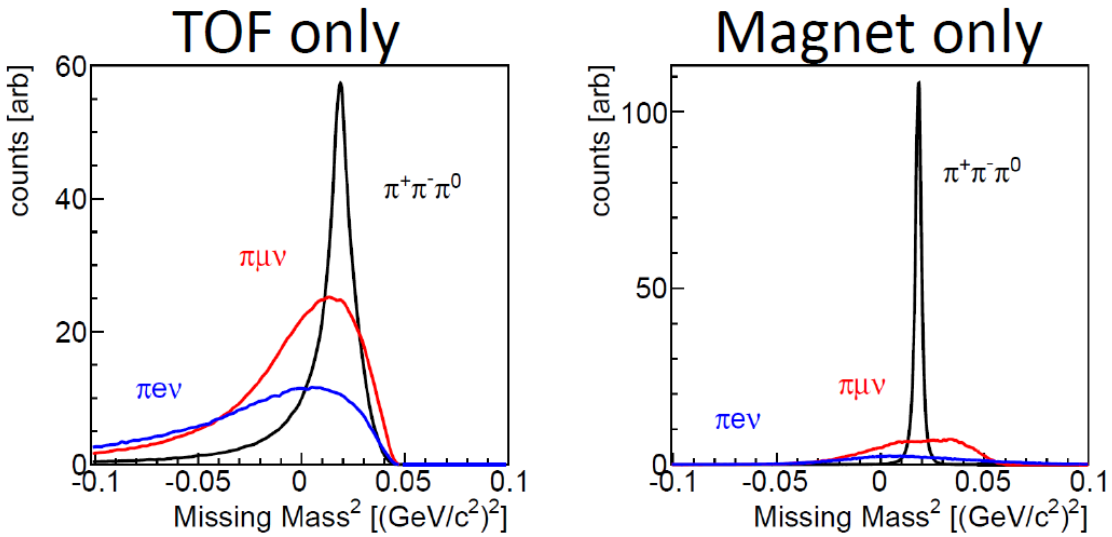

FIG. 14. Missing mass squared for the ToF and magnetic reconstruction of kaon decay.

Since the ratio between different branches is known extremely well, in the absence of additional backgrounds the ToF reconstruction is sufficient. In the presence of unknown background additional rejection using the particle identification

technique β/p might be useful. As expected, the magnetic field provides more precise event reconstruction.

A. Backgrounds at the GlueX Spectrometer

One of the essential conditions for the KFM was the absence of the KLF induced background on the main GlueX spectrometer. In particular there were concerns that KLF magnetic system may guide charged particles into a GlueX tracker. We have studied various aspects if a solenoidal magnetic field can induce additional background and if a dipole magnetic field from the pair spectrometer magnet, which in our design is used as a swiping magnet, can enhance such a background. It was found that the answer on both questions is No! A solenoidal magnetic field does not change the background at all. A presence of an MRI machine slightly reduces the background since it is served as a passive shielding. The pair spectrometer magnet, when operational, marginally decreases the level of the background by swiping away some charged particles which otherwise might end up in the GlueX spectrometer. In general, the influence of KFM on a GlueX background conditions is very small, since the background is dominantly due to kaons which decay further downstream.

VII. NEUTRON BACKGROUND

We do not expect any influence of the neutron background on the KFM. A similar system of ToF scintillators with trackers was working at the WASA detector for a decade under several orders of magnitude higher neutron fluxes without showing signal deterioration. Conventional PMT's proved to be very tolerable to a neutron flux. We also do not expect any substantial neutron backgrounds to the kaon flux measurements. At the position of the KFM assembly the neutron flux is more or less confined within the beam pipe. However, the divergence of the neutron beam will cause some charge particle background, which would be detected by the KFM. In some cases, like two-proton knockout or $nn \to pn\pi^-$ reactions in the beam pipe material, these events might mimic kaon decays. Fortunately, all these events would originate from the beampipe with a vertex displacement of a 35 mm in the transverse direction, which are well separated from real kaon decays. The KFM tracker system will provide sufficient accuracy to disentangle these cases with simple fiducial cuts. One also needs to take into account that kaons and neutrons are largely separated in time, see Figure 15. Neutron in tails from previous bunches are too slow to produce reactions with two charged tracks which can be misidentified with kaon decays. So in reality we need to care about many fewer neutrons which have similar velocities to kaons, and with vertex reconstruction and missing mass determination such events can be eliminated.

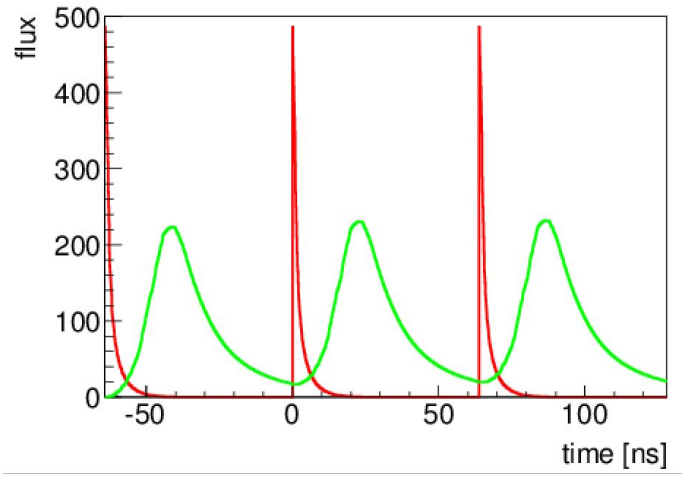

FIG. 15. Time structure of kaon (red) and neutron (green) fluxes.

VIII. ONLINE MONITORING

Kaon beam is produced in a two-step process ($e^- \to \gamma \to K_L$) with extremely large level arms between production stations. That is why it is important to monitor both position and momentum distribution of the kaon flux online, which can help to adjust electron beam properties when necessary.

Due to reasonably low count rate, we expect to perform a full event reconstruction online in event-by-event basis. In addition, we also plan to perform a "simplified" monitoring which would not require the full reconstruction and accurate calibration to get the basic information. Due to the cylindrical symmetry of the KFM start detector we expect uniform count rate over all elements. However, if a kaon beam would get some misalignment, we expect to see it immediately on the start counter detector rate.

The rough kaon momentum monitoring also do not require precise event reconstruction. Without tracking information the precise knowledge about kaon decay vertex is unavailable. However, we still know that it happen somewhere within 2 meters between the centre of the pair spectrometer magnet and a start detector. In a simplified monitoring routine we can assume that kaon decayed at location of start detector and that kaon time of flight is defined as a time difference between photon arrival time to a Be-target and an average time of two hits of start detector. Under these assumptions, we will get a following momentum resolution uncertainty, see Fig. 16(averaged over three 2-charged track decay channels).

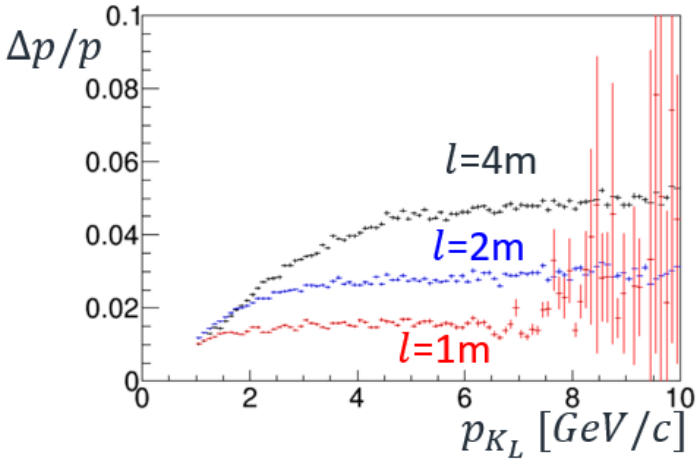

FIG. 16. Accuracy of simplified kaon momentum reconstruction without tracker. The length l correspond to a distance between the centre of pair spectrometer magnet and a Start detector.

A decent accuracy of ∼3% is achievable with proper calibration. However, since accounting for the light propagation time in the detector elements require tracking, an achievable time resolution will be a bit worse, which is 5–10%. This is still sufficient for the online monitoring and beam adjustments.

IX. EXISTING EQUIPMENT AND RELOCATION TIMELINE

As described above, in a benchmark design the KFM will consist of a time-of-flight system (KFM-TOF) and a tracker (KFMPC). Both parts of equipment re-utilise existing components of the WASA-at-COSY detectors. The KFM-TOF consist of two detectors, a Start detector (Forward Window Counter) and a Stop detector (Forward Veto hodoscope), designed and constructed at the University of Tübingen, Germany (PI - H. Clement and Co-PI - M. Bashkanov). A tracker was constructed at the University of Uppsala, Sweden (PI - T. Johansson). Currently both detectors are still installed at the COSY (Jülich, Germany) and will be available for relocation starting from Q4 2023. It was agreed with both university PI's and a Jülich research centre that these detectors and associated equipment can be used at KLF. Both detector system have dimensions (beam pipe hole diameter, distance from the beam pipe to the floor, active detector diameter) which fits KFM design very well and do not require any further modifications.

X. DECOMMISSIONING

Due to very small particle fluxes we expect negligible level of KFM activation, which should allow KFM decommissioning more or less immediately after the end of a beamtime. Removing of all KFM detector components is straightforward, and is expected to be done in less than a month time. The re-installation of the photon beam pair spectrometer, shielding wall, and associated beam line will require another month.

XI. COSTS

The University of York as a KFM PI requested £22k from upcoming UKRI consolidated grant (2024–2027) for relocation and commissioning of these systems (This comprises relocation (£10k), construction and commissioning of a new support system (£5k) and making a new readout DAQ [new DAQ computer + communication electronic] (£7k)). We have also requested 40% FTE PDRA to perform this relocation and 20% FTE technician.

Besides measuring kaon flux, KFM may significantly contribute to study of rare and CP-violating K_L-decays. One of the most rare, $Br \sim 10^{-9}$ K_L β-decay, will be a unique mode which can be accessed at KFM. To enable this optional part of the program we further requested (£100k) for purchasing an ex-MRI magnet (£85k) which will suffice to provide the solenoid magnetic field. We also requested shipping costs (£15k) and associated technical/PDRA support during its installation. We already got very positive responses from grant panel reviewers, however the final decision, including funding allocation, is pending.

XII. JLAB CONTRIBUTION

It is expected that JLab will provide cooling water ($\sim$ 40 l/min to 120 l/min) for the magnet, electricity ($\sim$ 15 kW) and organise mounting points for the new equipment. According to JLab engineering staff, all these additions are easily manageable.

No modifications of the platform is necessary in either the both magnet and no-magnet design. In a magnet design, the ex-MRI requirements on water and power supplies are very mild and can be easily fulfilled by the Hall. The MRI magnet cooling is expected to operate in a no-boil-off mode. In this case, according to the MRI specifications, the helium refill is expected to be once in 10 years. A replacement of a photon beamline to accommodate the larger diameter of the kaon beam is foreseen. The only two requirement from a KFM side - the use of low permeability stainless steel for the pipe to accommodate magnet design and the use of dedicated section with two flanges to simplify KFM installations - are incorporated in the engineering drawing, Fig 17.

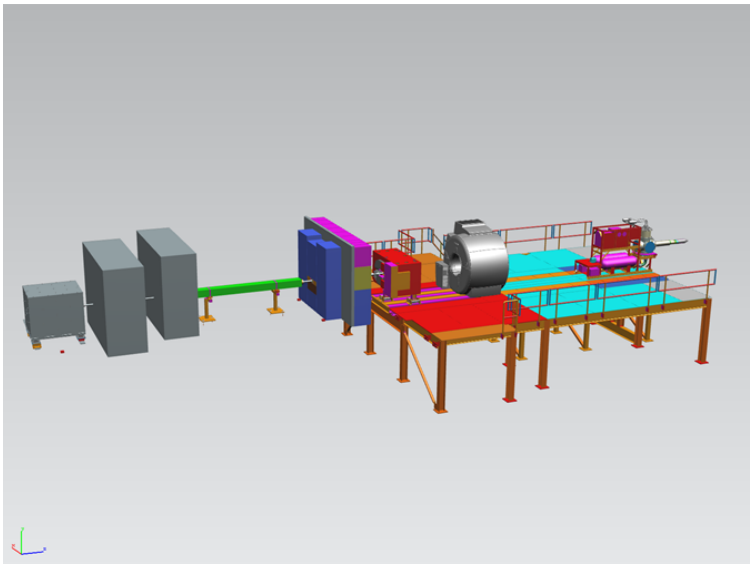

FIG. 17. Engineering drawing of a Hall-D with incorporated MRI magnet.

XIII. SUMMARY

The proposed Flux Monitor described above can determine the K_L flux with accuracy better than 5% over the full range of KLF energies. The construction is straightforward and can be completed within 1 year. No prototyping is necessary. The achievable reconstruction resolution is determined by the tracking system and TDC electronics. The overall cost of the KFM construction is very low. No interference with existing Hall-D equipment is expected.

XIV. APPENDIX A: CAD DRAWINGS

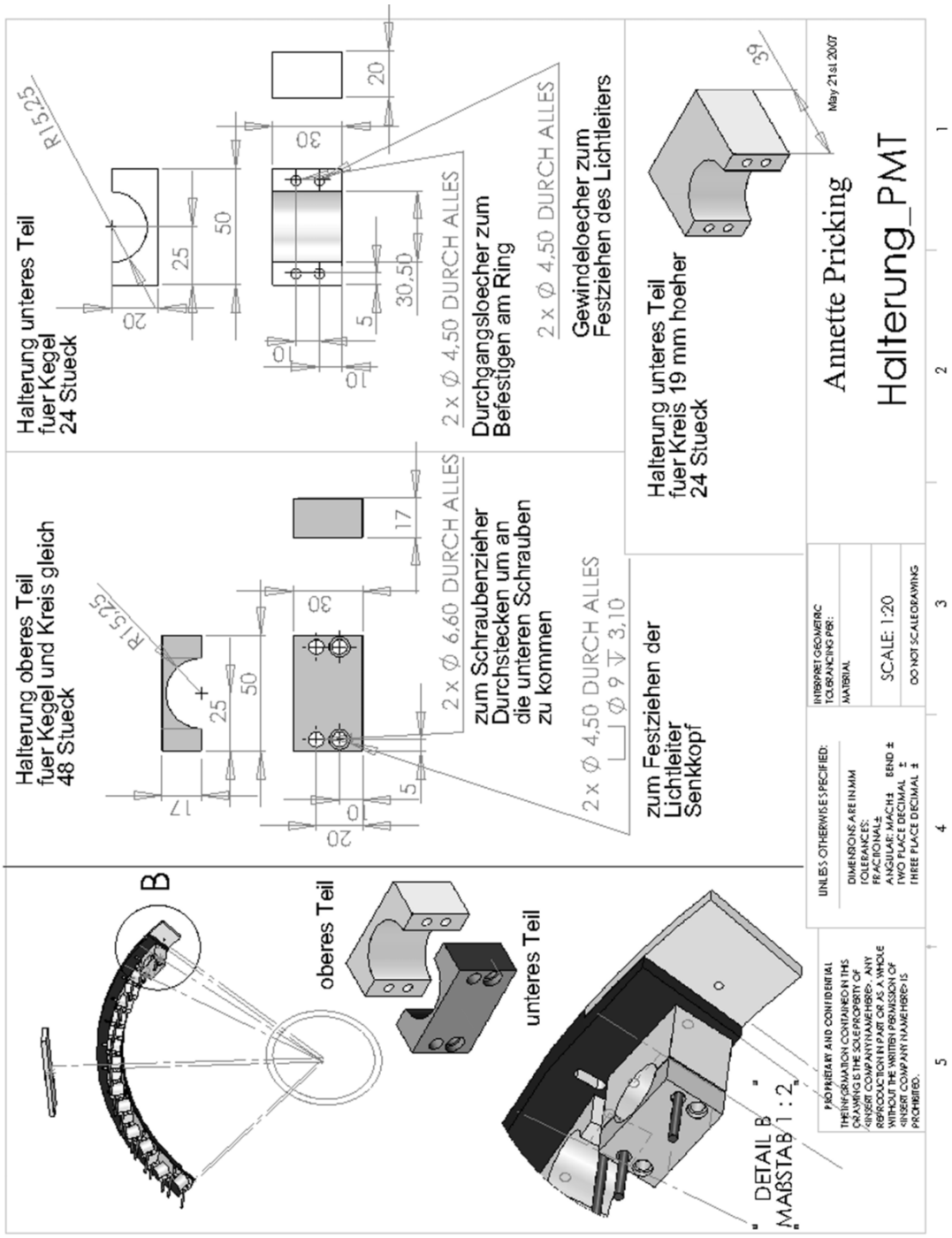

FIG. 18. Start detector mounting system CAD Drawing.

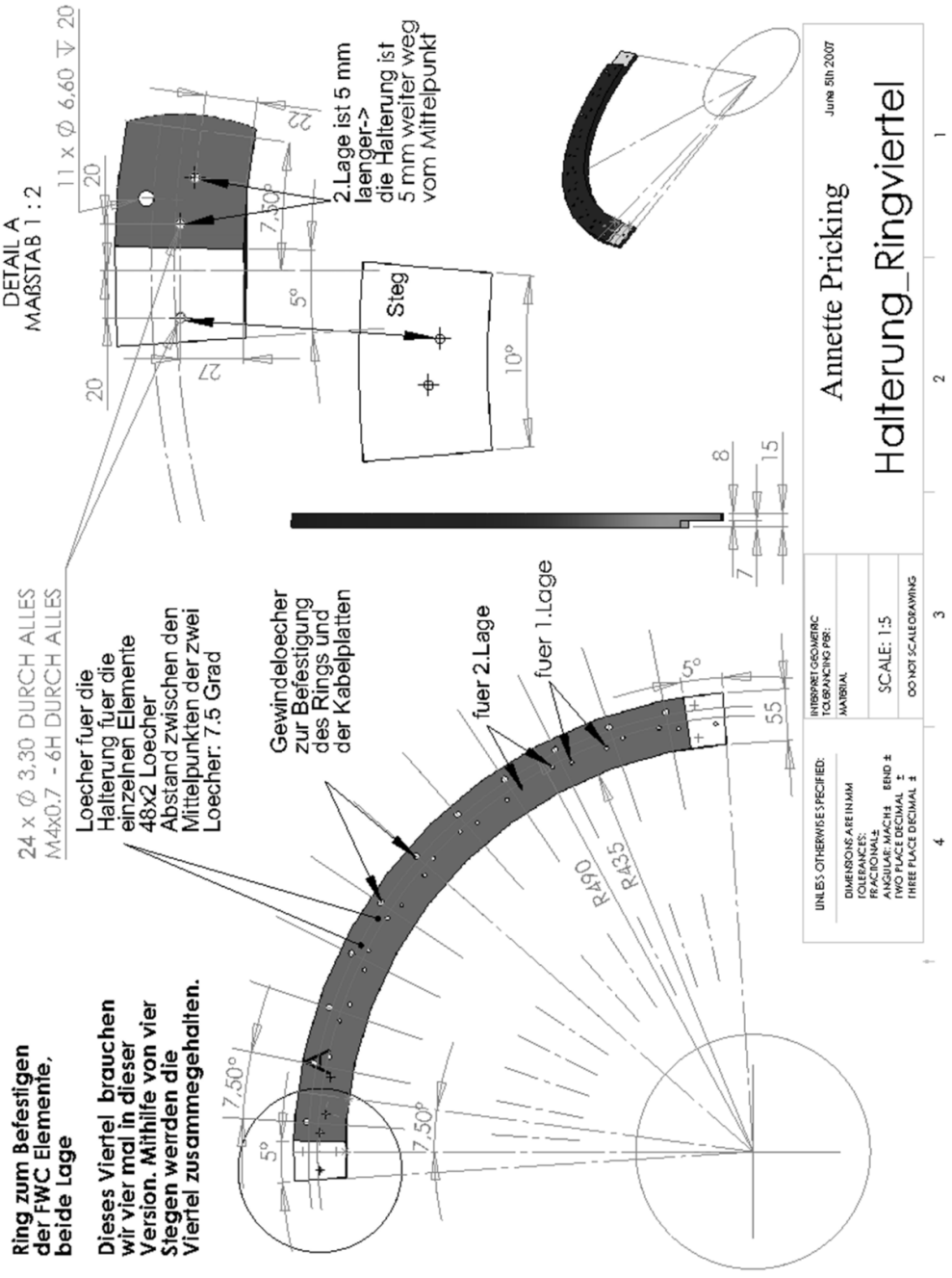

FIG. 19. Start detector support CAD Drawing.

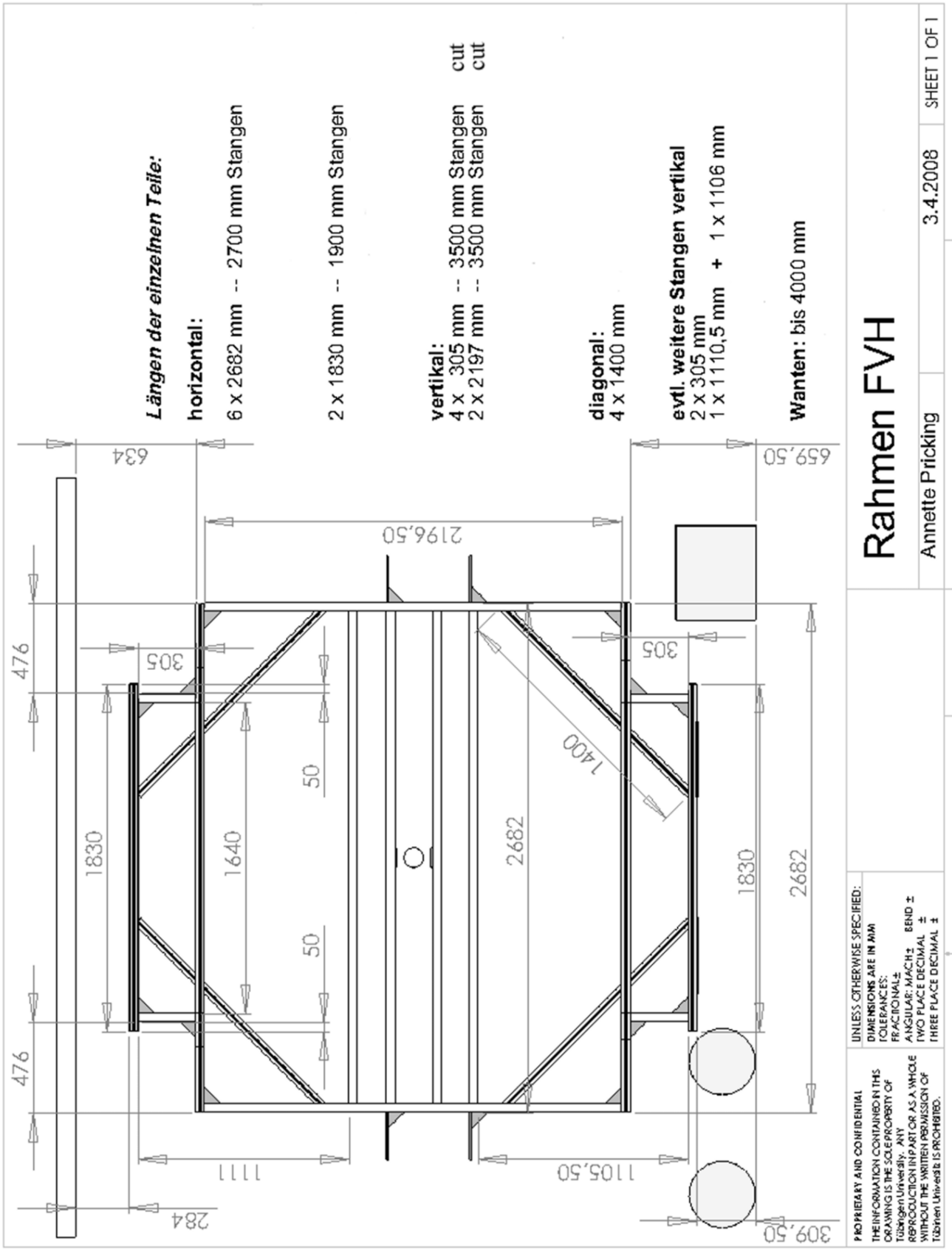

FIG. 20. Stop detector support structure CAD Drawing.

[1] M. G. Albrow, D. Aston, D. P. Barber, L. Bird, R. J. Ellison, C. Halliwell, A. E. Harckham, F. K. Löbinger, P. G. Murphy, J. Walters *et al.* "Photoproduction of k0 mesons from protons and from complex nuclei," Nucl. Phys. B **23**, 509 (1970).
[2] R. L. Workman *et al.* [Particle Data Group], "Review of Particle Physics," PTEP **2022**, 083C01 (2022).
[3] A. Pricking, "Double pionic fusion to ^{4}He," Ph.D. Thesis, Tübingen Univ., (2010); https://publikationen.uni-tuebingen.de/xmlui/handle/10900/49542 .
[4] H. H. Adam *et al.* [WASA-at-COSY Collaboration], "Proposal for the wide angle shower apparatus (WASA) at COSY-Jülich: WASA at COSY," [arXiv:nucl-ex/0411038 [nucl-ex]].
[5] H. Kleines *et al.* "Development of a high resolution TDC module for the WASA detector system based on the GPX ASIC," IEEE Nucl. Sci. Symposium Conf. Record, **30**, 1005 (2006).
[6] TDC-GPX Datasheet. Acam Messelectronic GMBH, 2006.
[7] H. Kleines, K. Zwoll, P. Wustner, W. Erven, P. Kammerling, G. Kemmerling, H. W. Lövenich, A. Ackens, M. Wolke, V. Hejny *et al.* "The new DAQ system for WASA-at-COSY," IEEE Trans. Nucl. Sci. **53**, 893 (2006).
[8] Each event has 8 time stamps 4 from Start detector and 4 from Stop one due to 2 charged track geometry.